Official URL: https://doi.org/10.1016/j.apsusc.2019.144357

To cite this version:

Fedoseeva, Yu.V. and Bulusheva, Lyubov Gennadievna and Koroteev, Victor O and Mevellec, Jean-Yves and Senkovskiy, Boris V and Flahaut, Emmanuel and Okotrub, Alexander Vladimirovich *Preferred attachment of fluorine near oxygen-containing groups on the surface of double-walled carbon nanotubes.* (2020) Applied Surface Science, 504. 144357. ISSN 0169-4332

Preferred attachment of fluorine near oxygen-containing groups on the surface of double-walled carbon nanotubes

Yu.V. Fedoseeva[a,b,*], L.G. Bulusheva[a,b], V.O. Koroteev[a,b], J.-Y. Mevellec[c], B.V. Senkovskiy[d,e], E. Flahaut[f], A.V. Okotrub[a,b]

[a] Nikolaev Institute of Inorganic Chemistry SB RAS, 3 Acad. Lavrentiev Ave., 630090 Novosibirsk, Russia
[b] Novosibirsk State University, 2 Pirogova Str., 630090 Novosibirsk, Russia
[c] Institut des Matériaux Jean-Rouxel (IMN), CNRS–UMR 6502, Université de Nantes, 2 rue de la Houssinière, BP 32229, 44322 Nantes Cedex 3, France
[d] St. Petersburg State University, 7-9, Universitetskaya Nab., St. Petersburg 199034, Russia
[e] II Physikalisches Institut, Universität zu Köln, Zülpicher Straße 77, 50937 Köln, Germany
[f] CIRIMAT, Université de Toulouse, CNRS, INPT, UPS, UMR CNRS-UPS-INP N°5085, Université Toulouse 3 Paul Sabatier, Bât. CIRIMAT, 118, route de Narbonne, 31062 Toulouse Cedex 9, France

ARTICLE INFO

Keywords:
Double-walled carbon nanotubes
Oxyfluorination
XPS
NEXAFS
DFT

ABSTRACT

Two samples of double-walled carbon nanotubes (DWCNTs), one with well-graphitized nanotube walls and another containing oxygen at outer nanotube surfaces, were fluorinated at room temperature using gaseous BrF_3. The products were comprehensively studied using transmission electron microscopy, Raman scattering, X-ray photoelectron, and near-edge X-ray absorption fine structure spectroscopies. The experimental data found twice the concentration of sidewall fluorine in the oxygenated DWCNTs. Quantum chemical modeling supported the experimental results revealing the preferable development of CF areas near the carbon atoms bonded with oxygen-containing groups. This observation demonstrates that tuning of the physical and chemical properties of carbon nanotubes can be achieved via the controlled co-modification by fluorine and oxygen functional groups.

1. Introduction

Carbon nanotubes (CNTs) are of great interest due to their outstanding mechanical, electrical, and optical properties, and they can be used in different applications [1]. Double-walled CNTs (DWCNTs) are the thinnest multi-walled CNTs (MWCNTs). In DWCNTs, inner shells have the properties typically found for SWCNTs, and the outer shells protect them from external influences, including strong oxidative conditions [2]. Oxygenation and fluorination are the most effective ways for chemical surface modification of CNTs. The attached functional groups improve the wettability and dispersibility of CNTs and change their optical and electrical properties. Co-modification of CNTs by oxygen and fluorine (oxyfluorination) opens the potential for the synthesis of chemical derivatives of DWCNTs with various functional properties of outer shells. It was shown that oxyfluorinated MWCNTs are hydrophilic, have good dispersibility in water, and can be used for oil–water separation [3]. Addition of oxyfluorinated MWCNTs to the polymer matrix was used to produce polymer composites with improved mechanical and electromagnetic shielding properties [4,5]. Polyaniline-coated oxyfluorinated MWCNT nanocomposites exhibited a high response for the detection of NH_3 gas [6]. Yu et al. demonstrated that oxyfluorinated MWCNTs have efficient glucose sensor properties [7]. Oxyfluorination of activated carbon resulted in enhancement of specific capacitance in electrical double layer capacitors [8]. This phenomenon was attributed to the synergistic effect of the high porosity of carbon material and electrochemically active surface functional groups, such as C—F and quinone C═O.

There are several methods for fluorine and oxygen co-addition to the surface of carbon materials. One of the most common ones is the use of a mixture of F_2 and O_2 gases for simultaneous covalent attachment of the fluorine and oxygen functionalities [3–12]. Concentrations of O and F in the oxyfluorinated samples depend on the ratio of F_2/O_2 gases in the reaction mixture, dilution by N_2 gas, and temperature of the reaction. This oxyfluorination reaction proceeds at room temperature without any initiator and catalyst [7] giving a product with concentrations of F and O up to 10 at% of each element [8,12]. Seo et al. [12] showed that a rise of the reaction temperature from 25 to 400 °C decreased the fluorine content in carbon fibers from 10 to 8 at% and increased the oxygen content from 6 to 10 at%. However, Park et al. obtained oxyfluorinated MWCNTs with a surface concentration of F and

---

* Corresponding author at: Nikolaev Institute of Inorganic Chemistry SB RAS, 3 Acad. Lavrentiev Ave., 630090 Novosibirsk, Russia.
E-mail address: fedoseeva@niic.nsc.ru (Y.V. Fedoseeva).

https://doi.org/10.1016/j.apsusc.2019.144357

O of about 2 3 wt% when the reaction temperature varied from 25 to 300 °C [11]. The highest concentrations of F (3.41 wt%) and O (2.27 wt %) were obtained at 100 °C [11]. The partial pressure of F_2 in the gas mixture also affects the composition of the synthesis product [4,7,8]. Liu et al. revealed that MWCNTs were grafted with two times less fluorine when F_2 was together with O_2 than when it was used alone under the same reaction conditions [3]. The authors suggested that F_2 might create reactive sites for O_2 on the MWCNTs surface. A higher reactivity of oxygen in the presence of fluorine was also demonstrated when CNT arrays were treated by plasma discharge of F_2 with residual O_2 [13]. The treatment resulted in covalent attachment of F atoms and a large amount of oxygen containing groups to the surface of CNT arrays.

Despite the advantages of one step preparation of oxyfluorinated CNTs, this method has some restrictions. Namely, since a high reaction temperature caused detachment of fluorine atoms and an increase in oxygen content, a high degree of fluorination of oxyfluorinated CNTs cannot be obtained [12,13]. Besides, when oxidation and fluorination processes coincide, it is challenging to determine the effect of a particular element in the process of oxyfluorination and to produce carbon samples with a given number and ratio of functional groups.

Oxyfluorinated CNTs can also be obtained by fluorination of oxygenated CNTs or by oxygenation of fluorinated CNTs. Unfortunately, it was shown that functionalization of fluorinated CNTs using urea or nitric acid causes their strong defluorination [14,15]. Direct fluorination of MWCNTs, which were previously oxidized by an H_2SO_4/HNO_3 mixture, resulted in only 3 at% of fluorine in the product. This product had the specific surface area and mesopore volume larger than those for initial MWCNTs [10]. Wang et al. produced fluorinated MWCNTs with a fluorine content of 9.2 at% after thermal treatment of oxidized MWCNTs by F_2 [16]. It was revealed that oxygen groups present on the MWCNT surface contributed to the formation of stronger covalent C—F bonds under fluorination at elevated temperatures. Direct fluorination of graphite oxides by pure F_2 gas or F_2/N_2 gas mixtures was also effectively used to produce oxyfluorinated graphite and graphene [17 21]. The samples had a higher concentration of fluorine than graphite fluorinated under the same conditions. As compared to graphite oxides, oxyfluorinated graphites showed a higher sensitivity to NH_3 gas [19,20], good water solubility [21], and better performances in primary lithium ion batteries [22].

Comprehensive works on a multiscale characterization of an atomic structure of oxyfluorinated DWCNTs are scarce in the literature. To fill the gap, in this paper, DWCNTs after two stage oxidative treatment by mineral acids and subsequent fluorination by a gaseous BrF_3 at room temperature have been investigated using a set of microscopic and spectroscopic techniques combined with quantum chemical modeling within density functional theory (DFT). Fluorination by BrF_3 at room temperature allows controlling the fluorine content in graphite [23,24], does not destroy the tubular morphology of carbon and keeps intact the inner tubes in DWCNTs and MWCNTs [25,26]. In contrast to fast fluorine action at elevated temperatures, which yields small compact CF areas, fluorination at room temperature during a long time produces short armchair or zigzag CF chains [24,26,27]. Here, fluorinated and oxyfluorinated DWCNTs have been comparatively studied using X ray photoelectron spectroscopy (XPS) and near edge X ray absorption fine structure (NEXAFS) spectroscopy methods. XPS probes the surface composition of a sample and chemical state of individual elements. This method is widely used for the study of chemically functionalized CNTs, including oxygenated and fluorinated ones [25,28 32]. Meanwhile, NEXAFS provides information about the partial density of unoccupied electronic states of elements. Previously, we have revealed that the shapes of NEXAFS F K edge and C K edge spectra of the fluorinated CNTs and graphite fluorides depend on the fluorine pattern developed on the graphitic network [26,33]. Since XPS and NEXAFS techniques are sensitive to the local chemical surrounding of atoms, they can be used in combination with quantum chemical modeling to identify the atomic structure of oxyfluorinated DWCNTs. The surface modification of CNTs through oxyfluorination can be used to modify the optical and luminescence properties. For example, unusual visible photoluminescence observed in the spectra of halogenated and oxidized CNTs has been arisen from small sp^2 carbon clusters, which are isolated from each other's by functional groups [34 36].

2. Experimental

2.1. *Materials*

DWCNTs were grown by catalytic chemical vapor deposition (CCVD) method using a mixture of methane (18 mol%) and hydrogen at 1000 °C and a Mo containing $Mg_{1\ x}Co_xO$ catalytic system [37], and purified from the MgO support by a concentrated aqueous HCl solution [38]. As shown by high resolution transmission electron microscopy (HRTEM), DWCNT sample consisted of *ca.* 80% DWCNTs, 20% SWCNTs, and traces of triple walled nanotubes. The outer diameter of the DWCNTs ranged from 1.2 to 3.2 nm, and the diameter of inner tubes varied from 0.5 to 2.5 nm. To remove amorphous carbon, which is deposited on the catalyst free surface of MgO [39], and non protected catalyst particles, the sample was annealed in air at 550 °C for 0.5 h followed by treatment with an aqueous solution of HCl (*ca.* 30%). This sample was denoted pDWCNTs. The pDWCNTs were oxidized using a two stage process widely studied by Bortolamiol et al. [40]. Firstly, a sample was refluxed in 3 M HNO_3 at 130 °C for 24 h and then treated by a mixture of 15 M HNO_3 and 18 M H_2SO_4 (volume ratio is 1:3) at 70 °C for 5 h. The oxidized sample, denoted ox DWCNTs, was washed by deionized water three times to neutral pH and dried at 100 °C for 24 h. Fluorination of ox DWCNTs and pDWCNTs was performed in a Teflon flask with gaseous BrF_3 diluted by vapors of Br_2 at room temperature for 3 days according to the method described in [41].

2.2. *Instrumentations*

Morphology and structure of samples were examined by transmission electron microscopy (TEM) on a JEOL 2010 microscope using 200 kV acceleration voltage and Raman scattering using a Renishaw Invia spectrometer with an excitation wavelength of 514 nm. The XPS and NEXAFS experiments were performed at the Berliner Elektronenspeicherring für Synchrotronstrahlung (BESSY II) using monochromatic radiation from the Russian German beamline. XPS spectra were measured using excitation energy of 830 eV with a resolution of 0.2 eV (full width at half maximum (FWHM)). XPS core line spectra were fitted employing the Casa software using Shirley backgrounds and Gaussian Lorentzian fitted peaks. The component at 284.5 eV in the C 1s spectra was fitted using the Doniach Sunjic high energy tail. NEXAFS spectra were acquired in a total electron yield mode. The spectra were normalized to the primary photon current from a purified gold foil.

2.3. *Calculations*

DFT calculations were carried out using the three parameter hybrid functional of Becke [42] and Lee Yang Parr correlation functional [43] (B3LYP method) included in the Jaguar package [44]. Atomic orbitals were described by the 6 31G* basis set. The nanotube surface was modeled by a fragment of an armchair (12,12) tube with a $C_{106}H_{28}$ composition, where hydrogen atoms saturated the dangling bonds of boundary carbon atoms. Fluorine and oxygen containing groups decorated the central convex part of the tube fragment to model fluorinated and oxyfluorinated carbon surfaces. Positions of carbon and hydrogen atoms at the segment edges were frozen during optimization of the models. The structure relaxation was conducted using an analytical method to the gradient of 5×10^{-4} atomic units for atom displacements.

Theoretical NEXAFS F K spectra were constructed within the (Z + 1) approximation [45], which accounts for the effect of a final core hole created in the absorption process on the spectral profile. In order to model a core hole, the excited atom was replaced by the element being next in the periodic table and, in the case of fluorine, this is Ne. For compensation of the extra electron, the model was charged positively. Compared to the full core hole calculations, the (Z + 1) approximation requires significantly fewer computer resources and well fits NEXAFS C K and F K spectra of fullerene C_{60}, CNTs, graphite and their derivatives [26,29,46,47]. Intensities of the spectral lines were obtained by summing the squared coefficients at the Ne 2*p* orbitals and broadened with Lorentzian functions of a width of 0.7 eV. X ray transition energies were determined as a difference between Kohn Sham eigenvalues of virtual molecular orbitals of a model calculated within the (Z + 1) approximation (excited system) and the 1*s* level energy of fluorine in the ground state of that model.

3. Results and discussion

Typical TEM images of air purified DWCNTs (pDWCNTs), acid purified/oxidized DWCNTs (ox DWCNTs) and these samples after fluorination (F pDWCNTs and F ox DWCNTs) are presented in Fig. 1. The first sample consists of clean DWCNTs with no visible impurities of amorphous carbon by products or carbon encapsulated catalytic metallic particles (Fig. 1a), which are commonly formed during the CCVD synthesis and present in the as grown material [38]. It means that the purification by oxidation in air removes almost all the amorphous carbon impurities. TEM analysis of ox DWCNTs highlighted carbon deposits on the nanotube surface (indicated by arrows in Fig. 1b). It should be noted that in previous works oxidation of nanotubes, opening of nanotube's tips and formation of defects were discovered after oxidative treatments with concentrated nitric and sulphuric acids [35,36,40]. Such functionalized nanotubes are less stable and can be partially broken under the electron beam during the TEM observation with the formation of surface carbon clusters. The tubular structure of the pDWCNTs and ox DWCNTs was preserved after the fluorination (Fig. 1c, d). However, at the visual inspection, it seems that amounts of sidewall carbon clusters and defects increases, especially in the oxyfluorinated sample denoted F ox DWCNTs (Fig. 1d). We assume that further destructions observed for the fluorinated samples are the result of the electron beam effect, which has been previously observed for highly fluorinated SWCNTs [48]. Oxyfluorinated DWCNTs appear to be less stable, probably due to a higher concentration of fluorine surface groups.

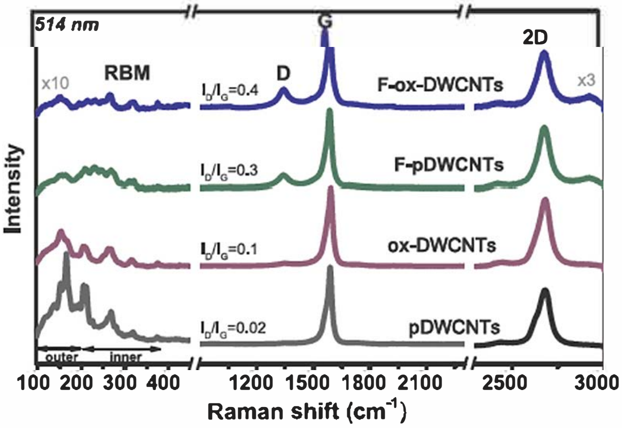

Fig. 2. Raman spectra at 514 nm excitation wavelength of pDWCNTs and ox-DWCNTs before and after fluorination (F-pDWCNTs and F-ox-DWCNTs).

Fig. 2 compares the Raman spectra of the samples. The spectra are typical for DWCNTs, showing radial breathing modes (RBM) in the region of 100 400cm^{-1}, a sharp tangential mode G at ~1586 cm^{-1}, a

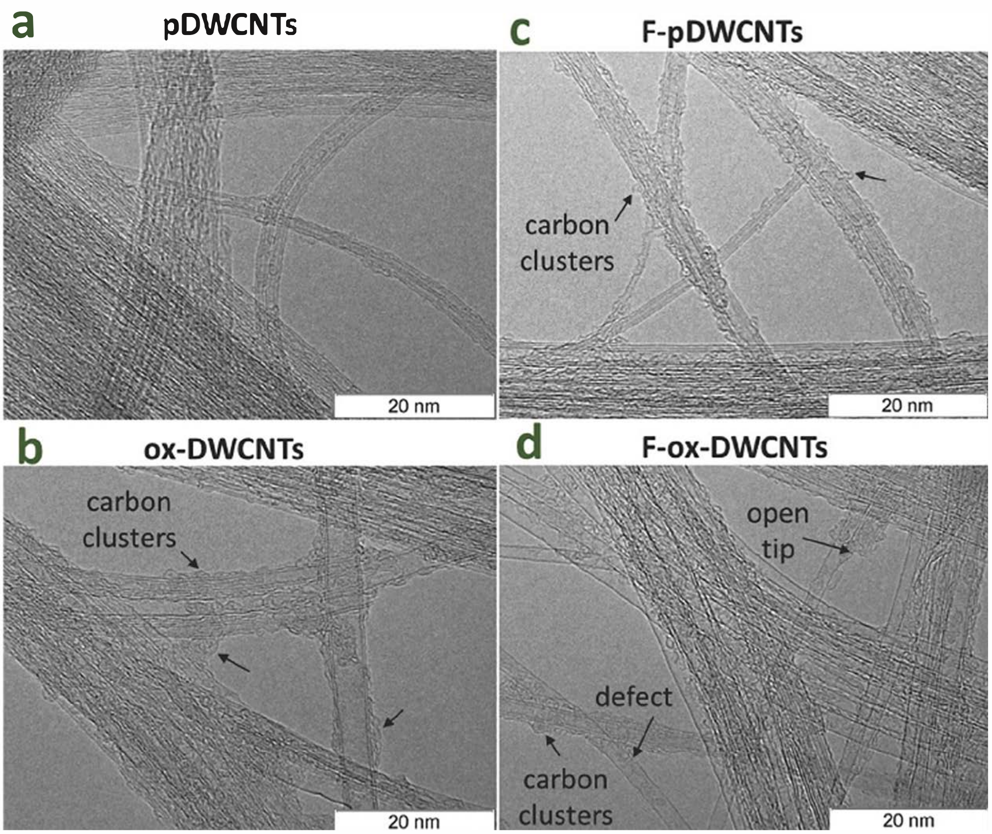

Fig. 1. TEM images of air-purified DWCNTs (a, pDWCNTs), oxidized/purified DWCNTs (b, ox-DWCNTs), fluorinated pDWCNTs (c, F-pDWCNTs) and fluorinated ox-DWCNTs (d, F-ox-DWCNTs).

disorder-induced mode D at 1350 $\mathrm{cm^{-1}}$, and a two-phonon 2D band at 2680 $\mathrm{cm^{-1}}$ [49]. The integral ratio of the intensities of D mode to G mode (I_D/I_G) in the Raman spectrum of pDWCNTs was equal to 0.02. This low value indicates that the air-purified DWCNTs have a long-range sp^2 hybridized carbon order along sidewalls and a small amount of graphene-like carbon contaminations. The frequency positions of the RBM peaks allow us to analyze the distribution of diameters of the DWCNTs, which are excited at 514 nm. According to the relations $\omega_{RBM}(\mathrm{cm^{-1}}) = 228/d(\mathrm{nm})$ for the inner tubes, and $\omega_{RBM}(\mathrm{cm^{-1}}) = 204/d(\mathrm{nm}) + 27(\mathrm{cm^{-1}})$ for the outer tubes, where ω_{RBM} is the position of RBM peak and d is the diameter of a nanotube [50], we calculated the corresponding values in ranges of 0.6–1.1 nm and 1.5–1.8 nm. The spectrum of ox-DWCNTs exhibited the D mode with a slightly higher intensity ($I_D/I_G = 0.1$) and RBM peaks with intensities less than those for pDWCNTs. These changes indicate that acidic oxidative treatments produce some structural defects or/and functional groups on sidewalls of DWCNTs.

An increase in the intensity of the D peak in the Raman spectra of the fluorinated samples (I_D/I_G ratio is 0.3 for F-pDWCNTs and 0.4 for F-ox-DWCNTs) points out that DWCNTs are chemically functionalized by fluorine. The formation of C–F bonds also resulted in a decrease in the intensity of RBM peaks. The strongest spectral changes observed for oxyfluorinated DWCNTs indicate the highest degree of the modification. The 2D peak in the spectrum of pDWCNTs has a broad asymmetric shape due to the averaging series of individual 2D peaks from nanotubes with different (n,m) configurations [51–53]. The shape of the 2D peak changed slightly after both oxidation and fluorination of the sample. That phenomenon can be explained by changes in the structure of the π-electron system after the chemical modification. The ratio I_{2D}/I_G was 0.4 for pDWCNTs, ox-DWCNTs, and F-pDWCNTs and it decreased to 0.3 for F-ox-DWCNTs, meaning that the decrease in resonance from part of the nanotubes was due to the high degree of functionalization.

XPS survey spectra of the samples revealed signals from carbon, oxygen, copper from substrates, and fluorine atoms in the case of fluorinated samples (Fig. S1 in Supporting Information). Chemical states of carbon in the samples were revealed from the analysis of C 1s spectra, which were fitted by five components (Fig. 3). The spectrum of pDWCNTs has an asymmetric peak at 284.5 eV, characteristic of sp^2 hybridized carbon (Fig. 3a). A weak component C_d at 285.3 eV refers to disordered carbon and surface defect states [54]. According to low I_D/I_G intensity in the Raman spectrum of this sample, the residual amorphous carbon is likely not aromatic but tetrahedral with a high content of sp^3 bonding and/or hydrogen [55]. Moreover, defect states in the DWCNT walls may be considered as an intermediate between the sp^2 and sp^3 states and can also contribute to the component C_d at 285.3 eV. The peak at 286.3 eV corresponds to carbon atoms bonded with one oxygen atom (C–O) in hydroxyl, ether, epoxy, or other oxygen-containing groups [30,56,57]. The integral intensity of this peak is *ca.* 3% of the total spectral intensity. The peak at 288.3 eV arises from carbon atoms bonded with two oxygen atoms ($\mathrm{C{-}O_2}$) in carboxyl groups located at edges of vacancy defects and graphene layers [30,56–58]. The intensity of this peak is three times less than the intensity of the C–O component. The $\pi \rightarrow \pi^*$ electron transitions produce a satellite peak at 291.3 eV.

The C 1s XPS spectrum of ox-DWCNTs (Fig. 3b) showed the sp^2 and C_d components of the shape and intensity similar to those in the spectrum of pDWCNTs. That means that the used acidic treatment did not lead to noticeable destruction of the DWCNTs. On the other hand, such oxidation treatment caused the covalent functionalization of DWCNTs as can be seen from an increase in the intensities of the C–O and $\mathrm{C{-}O_2}$ components. The intensity of the former component is three times greater than the latter one. Commonly, treatment with concentrated nitric and sulphuric acids increases the content of carboxylic groups in the CNT samples [59–61]. Most of these groups are mainly located at the edges of small carboxylated carbon fragments, which appear as a result of oxidation of carbon graphene-like impurities. Almost all these fragments were removed by oxidation of the DWCNT sample in air before the acidic treatment (Fig. 1a); thus the carboxylic groups detected by XPS were most likely located at the open nanotube edges. Analysis of O 1s XPS and NEXAFS O K-edge spectra detected the presence of different oxygen-containing groups in the samples (Fig. S2 in

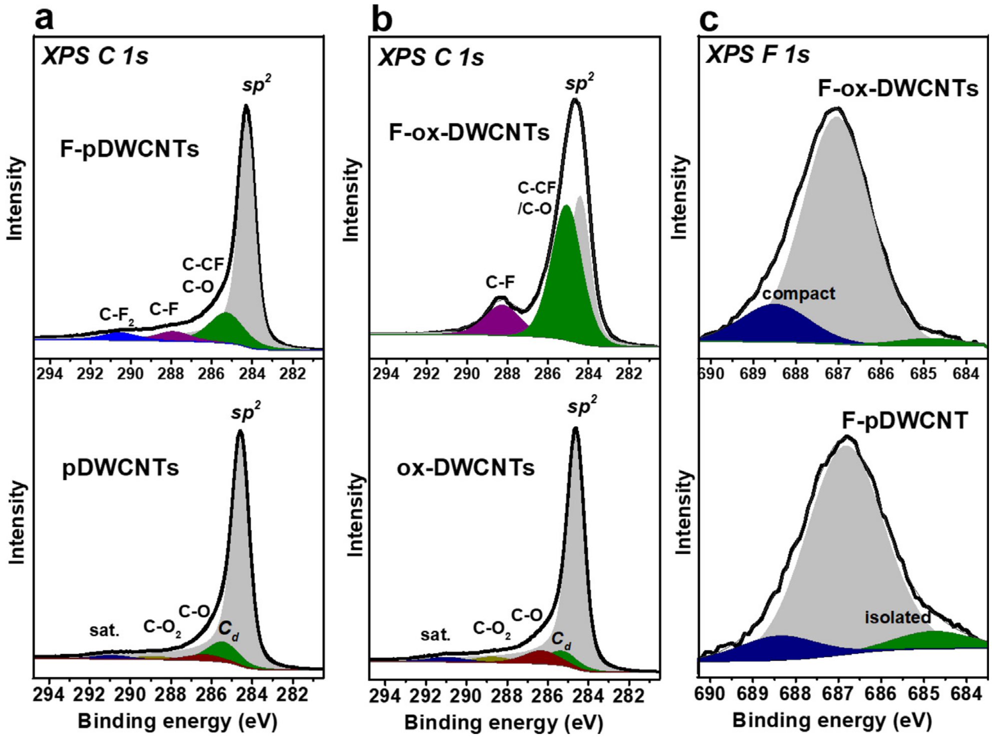

Fig. 3. C 1s XPS spectra of pDWCNTs and ox-DWCNTs before and after fluorination (F-pDWCNTs and F-ox-DWCNTs) (a, b). F 1s XPS spectra of F-pDWCNT and F-ox-DWCNT (c). Compact and isolated CF areas give eponymous components in the F 1s spectra (c).

Supporting Information). These spectra confirm that the C—O bonding prevails in the ox DWCNTs.

Two peaks at 288.4 and 290.6 eV were distinguished in C 1s XPS spectra of fluorinated samples (Fig. 3a,b). The peak at 288.4 eV corresponds to carbon atoms covalently bonded with one fluorine atom (C—F), which is located on the outer surface of CNTs [13,26,30]. The peak at 290.6 eV arises from carbon atoms covalently bonded to two fluorine atoms (C—F_2). These groups are more probably located at open nanotube tips. Carbon atoms linked with CF groups (C—CF) give a contribution to the component at 285.5 eV. For F pDWCNTs, areas of the C—F and C—F_2 peaks were 5% and 4%, respectively. In the spectrum of F ox DWCNTs, the C—F_2 peak was absent, and the area of the C—F peak was 11%. The fitting of the C 1s spectra gives compositions $(CF_{0.05})_{0.96}(CF_2)_{0.04}$ for sample F pDWCNT and $CF_{0.11}$ for sample F ox DWCNTs. The more significant number of CF_2 groups in pDWCNTs was likely formed at the DWCNT ends opened after annealing in air. In the F ox DWCNTs, these sites were probably initially occupied by oxygen containing groups during the treatment by acids. However, the concentration of sidewall fluorine atoms in F ox DWCNTs was two times higher than that in F pDWCNTs.

The chemical state of fluorine was identified from the analysis of F 1s lines, which were fitted by three components. Fig. 3c compares the F 1s XPS spectra for F pDWCNTs and F ox DWCNTs. The binding energy of F 1s levels of the fluorinated CNTs was lower than that for graphite fluorides CF and C_2F [62]. The F 1s peak shifted toward higher binding energy with fluorine loading as experimentally shown [50]. We tentatively approximated the F 1s spectra by three components at 688.4, 686.9, and 684.7 eV, which all belong to the covalent C—F bonds. The component at low energy of 684.7 eV indicates a weakly bonded F atoms [24]. According to quantum chemical calculations, the weakening of C—F bonding is observed when a fluorine atom locates far from other fluorinated carbon atoms and is caused by overlapping of electrons of the F atom with the π system of bare carbon regions [26,63,64]. The high energy F 1s component at 688.4 eV, on the contrary, can be assigned to the F atoms strongly interacting with carbon in the highly fluorinated CF areas and the edge CF_2 groups [26,50,65]. An intense intermediate peak at 686.9 eV refers to all other fluorine patterns. Comparison of the spectra indicates that F pDWCNTs contain a larger number of the isolated CF groups and F ox DWCNTs are enriched with compact CF areas.

NEXAFS C K edge spectra of the samples had two main resonances at 285.4 eV and 292.0 eV (Fig. 4) corresponding to $1s \rightarrow \pi^*$ and $1s \rightarrow \sigma^*$ transitions, respectively [49,58]. The features located between π* and σ* resonances refer to the carbon atoms bound to oxygen and fluorine [26,27,33,66]. The high intensity and a sharpness of the π* and σ* resonances in the spectrum of pDWCNTs indicates a perfect atomic structure of the nanotubes (Fig. 4a). The spectrum of ox DWCNTs showed a quite strong feature at 288.8 eV (Fig. 4b) formed by oxygenated carbon species [58,66]. The spectra of the fluorinated samples differ from the spectra of parent samples by the features between 287 and 290 eV due to covalent C—F bonding. High relative intensity of the π* resonance and weak intensity of the C—F/C—O features in the spectrum of F pDWCNTs (Fig. 4a) are due to a low sidewall fluorination level of the nanotubes. In contrast to this result, the spectrum of F ox DWCNTs exhibited a substantial decrease in the intensity of π* resonance and an increase in the intensity at 287 290 eV (Fig. 4b). These spectral changes mean that fluorine atoms are covalently attached to the surface of oxidized DWCNTs with broken of the conjugated π electron system.

Previously we showed that NEXAFS F K edge spectra are sensitive to the fluorine pattern and number, position, and intensity of pre edge features may vary depending on the fluorination method [26,27]. The F K edge spectra of the fluorinated DWCNTs exhibited two shoulders A and B at *ca.* 689.0 and *ca.* 686.5 eV in the region before the adsorption edge C (Fig. 5a). These pre edge features come from fluorine atoms, which form short fluorinated chains on the surface of CNTs [26]. Despite the higher concentration of fluorine in the oxyfluorinated sample, features A and B have lower intensities than those in the spectrum of the fluorinated sample (Fig. 5a).

To reveal the influence of basal and edge oxygen containing groups on the electronic state of fluorine, we performed the DFT calculations of the models presented in Fig. 5b. We used a fragment of (12,12) tube as a model of the non modified surface of pDWCNTs. Since the used fluorination method produces short CF chains [24,26,27], four F atoms forming a zigzag chain in the central convex part of the tube fragment were used for modeling of a fluorinated tube (model 1). The acidic oxidation of DWCNTs can produce only hydroxyl groups covalently grafted to sidewalls. A hydroxyl group replaced one edge F atom in the fluorinated model 1 to get the model 2 of oxyfluorinated DWCNTs. The edges of defects and open DWCNT tips, appeared during the oxidation, can be modified by —COOH and C—O—C groups. According to the XPS data, the concentration of —COOH groups was very low in the ox DWCNTs sample, and therefore, we did not consider the fluorinated models with these groups. Moreover, ether groups located at the edges

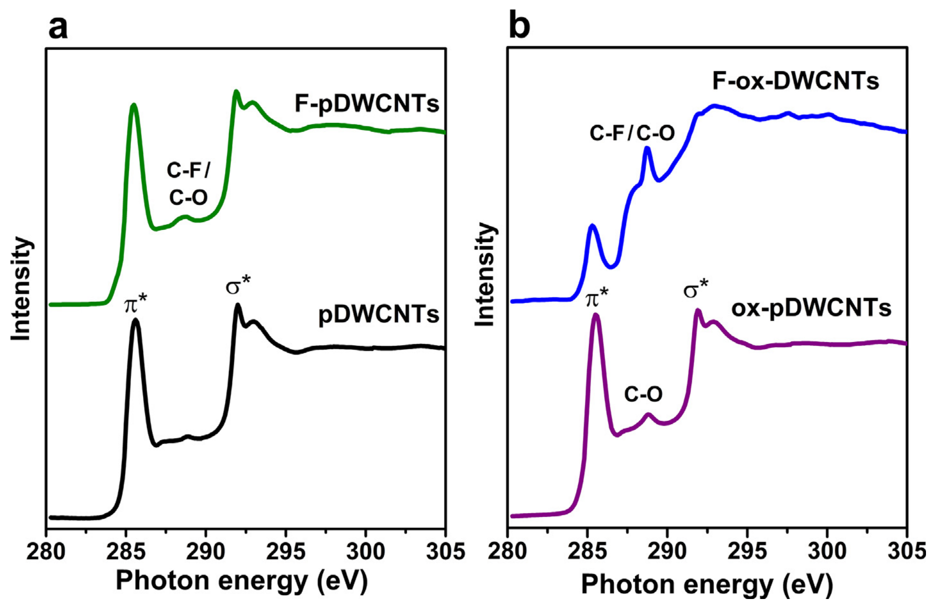

Fig. 4. NEXAFS C K-edge spectra of pDWCNTs (a) and ox-DWCNTs (b) before and after fluorination (F-pDWCNTs and F-ox-DWCNTs).

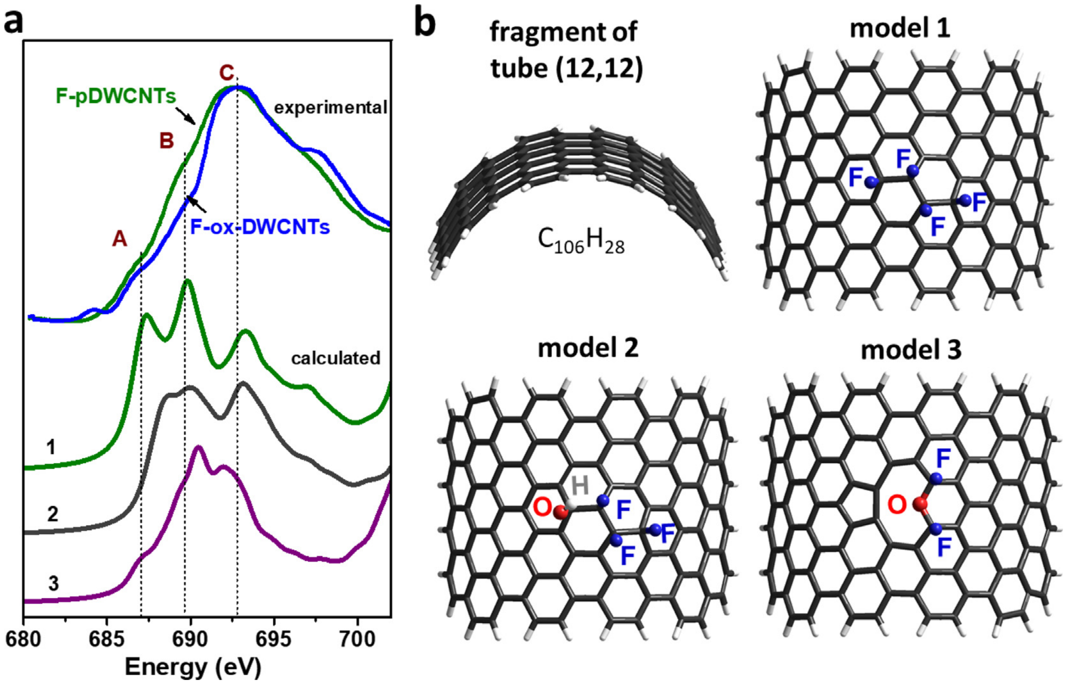

Fig. 5. Experimental NEXAFS F K-edge spectra of F-pDWCNTs and F-ox-DWCNTs in comparison with calculated spectra (1–3) constructed for fluorine atoms in the models 1–3 (a). Fragment of the tube (12, 12), and the fragments of the tube with fluorinated (model 1) and oxyfluorinated (models 2 and 3) central convex part (b).

of graphene planes were shown to be the most stable under fluorination [18]. We placed an O atom bonded to two fluorinated C atoms at the edge of a double atomic vacancy in model 3.

Fig. 5a shows the theoretical F K spectra plotted for all fluorine atoms in models 1 3 using (Z + 1) approximation. The spectrum of the fluorinated model 1 has three peaks, which coincide in related intensity and energy with the features A C in the experimental spectrum. The spectra of the two oxyfluorinated models 2 and 3 show a strong decrease in the intensity of peak A as well as a small decrease of peak B. These spectral changes correlate with the experimental ones observed for F pDWCNTs and F ox DWCNTs. Since carbon p_z orbital is required for sidewall fluorine attachment and the perfect π system is not easily destroyed, the reaction may start from the C atoms located near oxygenated carbon atoms. The attachment of oxygen weakens the neighboring C═C bonds, thus improving their reactivity to fluorine. We suggest that in our oxyfluorinated sample, the CF areas are compact and located near the carbon atoms bonded with oxygen groups.

Previously, the investigation of reactivity of graphene oxides to fluorination by F_2 gas at elevated temperatures revealed that oxygen groups promote fluorination reaction and formation of covalent C—F bonds [18]. Moreover, Chen and colleagues [18] found that the concentration of oxygen containing groups decreased during the high temperature fluorination and concluded that F radicals replaced carbonyl and hydroxyl groups and only ether groups resisted the high temperature and the attack of fluorine radicals. In our case, the concentration of sidewall oxygen in the ox DWCNTs was not so high, and F atoms were rather attached to the non functionalized C atoms than replacing oxygen containing groups. The same way that fluorine gas initiates the reaction of MWCNTs with oxygen during one step oxyfluorination [3], oxidized carbon atoms, already presented on the surfaces and edges of DWCNTs, become reactive sites for the fluorination of neighboring carbon areas.

4. Conclusion

DWCNTs, purified by heating in air (sample pDWCNTs) and the oxidative acidic media (sample ox DWCNTs), were compared under fluorination by gaseous BrF_3 at room temperature. TEM, Raman scattering, XPS, and NEXAFS measurements examined the composition and atomic structure of the initial and fluorinated samples. The use of purified DWCNTs is important to make sure that the fluorination occurred only on a CNT and not on other carbon species, such as amorphous carbon. The analysis of the XPS data found *ca.* 2 at% of oxygen in the pDWCNTs mainly in carboxylic groups and *ca.* 12 at% of oxygen in the ox DWCNTs mostly in the sidewall groups. Fluorination of the former sample yielded 5 at% of fluorine covalently bonded with carbon (C F) and 8 at% of fluorine in the edge CF_2 groups. Only sidewall fluorination (*ca.* 11 at%) was detected for the fluorinated ox DWCNTs. A comparison of experimental NEXAFS F K edge spectra with the spectra plotted using the DFT calculations of models revealed that fluorine is preferentially attached near the oxygen containing groups on the nanotube surface. Even a small number of oxygen containing groups covalently bonded to DWCNTs promotes the formation of many fluorinated areas, which cumulate near oxidized carbon. This observation may explain the difference observed and reported in the concentration of fluorine in the fluorinated CNTs and other carbon materials, which are obtained under the same fluorination conditions. The presence of a small concentration of oxygen should be taken into account in the further chemical modification of CNTs and other carbon materials.

Declaration of Competing Interest

The authors declare that they have no known competing financial interests or personal relationships that could have appeared to influence the work reported in this paper.

Acknowledgements

We are grateful to Mr. A.V. Ishchenko for the TEM measurements. The work has been supported by the Russian Foundation for Basic Research (Grant № 16 53 150003) and PRC CNRS/RFBR (Grant № 1023) and the bilateral Program “Russian German Laboratory at BESSY” in the part of XPS and NEXAFS measurements.

Appendix A. Supplementary material

Supplementary data to this article can be found online at https://doi.org/10.1016/j.apsusc.2019.144357.

References

[1] M. Monthioux, E. Flahaut, C. Laurent, W. Escoffier, B. Raquet, W. Bacsa, et al., Properties of carbon nanotubes, in: B. Bhushan, D. Luo, S.R. Schricker, W. Sigmund, S. Zauscher (Eds.), Handbook of Nanomaterials Properties, Springer Materials, Berlin, 2014, pp. 1–49.

[2] T. Hayashi, D. Shimamoto, Y.A. Kim, H. Muramatsu, F. Okino, H. Touhara, et al., Selective optical property modification of double-walled carbon nanotubes by fluorination, ACS Nano 2 (3) (2008) 485–488.

[3] Y. Liu, X. Wang, W. Wang, B. Li, P. Wu, M. Ren, et al., One-step preparation of oxygen/fluorine dual functional MWCNTs with good water dispersibility by the initiation of fluorine gas, ACS Appl. Mater. Interfaces 8 (2016) 7991–7999.

[4] K.M. Lee, S.-E. Lee, Y.-S. Lee, Improved mechanical and electromagnetic interference shielding properties of epoxy composites through the introduction of oxyfluorinated multiwalled carbon nanotubes, J. Ind. Eng. Chem. 56 (2017) 435–442.

[5] J. Yun, J.S. Im, Y.-S. Lee, H.-I. Kim, Effect of oxyfluorination on electromagnetic interference shielding behavior of MWCNT/PVA/PAAc composite microcapsules, Eur. Polym. J. 46 (2010) 900–909.

[6] J. Yun, J.S. Im, H.-I. Kim, Y.-S. Lee, Effect of oxyfluorination on gas sensing behavior of polyaniline-coated multi-walled carbon nanotubes, Appl. Surf. Sci. 258 (2012) 3462–3468.

[7] H.-R. Yu, J.G. Kim, J.S. Im, T.-S. Bae, Y.-S. Lee, Effects of oxyfluorination on a multi-walled carbon nanotube electrode for a high-performance glucose sensor, J. Ind. Eng. Chem. 18 (2012) 674–679.

[8] M.-J. Jung, E. Jeong, J.W. Lim, S.I. Lee, Y.-S. Lee, Physico-chemical surface modification of activated carbon by oxyfluorination and its electrochemical characterization, Colloids Surf. A: Physicochem. Eng. Asp. 389 (2011) 274–280.

[9] Y.-S. Lee, Syntheses and properties of fluorinated carbon materials, J. Fluor. Chem. 128 (2007) 392–403.

[10] S.D. Kim, J.W. Kim, J.S. Im, Y.H. Kim, Y.S. Lee, A comparative study on properties of multi-walled carbon nanotubes (MWCNTs) modified with acids and oxyfluorination, J. Fluor. Chem. 128 (2007) 60–64.

[11] S.-J. Park, H.-J. Jeong, C. Nah, A study of oxyfluorination of multi-walled carbon nanotubes on mechanical interfacial properties of epoxy matrix nanocomposites, Mat. Sci. Eng. A 385 (2004) 13–16.

[12] M.-K. Seo, S.-J. Park, Surface characteristics of carbon fibers modified by direct oxyfluorination, J. Colloid Interf. Sci. 330 (2009) 237–242.

[13] C. Struzzi, M. Scardamaglia, A. Hemberg, L. Petaccia, J.-F. Colomer, R. Snyders, et al., Plasma fluorination of vertically aligned carbon nanotubes: functionalization and thermal stability, Beilstein J. Nanotechnol. 6 (2015) 2263–2271.

[14] F. Chamssedine, D. Claves, Selective substitution of fluorine atoms grafted to the surface of carbon nanotubes and application to an oxyfluorination strategy, Carbon 46 (2008) 957–962.

[15] M.X. Pulikkathara, O.V. Kuznetsov, V.N. Khabashesku, Sidewall covalent functionalization of single wall carbon nanotubes through reactions of fluoronanotubes with urea, guanidine, and thiourea, Chem. Mater. 20 (2008) 2685–2695.

[16] X. Wang, Y. Chen, Y. Dai, Q. Wang, J. Gao, J. Huang, et al., Preparing highly fluorinated multiwall carbon nanotube by direct heating-fluorination during the elimination of oxygen-related groups, J. Phys. Chem. C 117 (2013) 12078–12085.

[17] M.-S. Park, Y.-S. Lee, Functionalization of graphene oxide by fluorination and its characteristics, J. Fluor. Chem. 182 (2016) 91–97.

[18] T. Chen, X. Wang, Y. Liu, B. Li, Z. Cheng, Z. Wang, et al., Effects of the oxygenic groups on the mechanism of fluorination of graphene oxide and its structure, Phys. Chem. Chem. Phys. 19 (2017) 5504–5512.

[19] M.-S. Park, K.H. Kim, M.-J. Kim, Y.-S. Lee, NH_3 gas sensing properties of a gas sensor based on fluorinated graphene oxide, Colloids Surf. A: Physicochem. Eng. Asp. 490 (2016) 104–109.

[20] V.I. Sysoev, A.V. Okotrub, I.P. Asanov, P.N. Gevko, L.G. Bulusheva, Advantage of graphene fluorination instead of oxygenation for restorable adsorption of gaseous ammonia and nitrogen dioxide, Carbon 118 (2017) 225–232.

[21] O. Jankovský, P. Šimek, D. Sedmidubský, S. Matějková, Z. Janoušek, F. Šembera, et al., Water-soluble highly fluorinated graphite oxide, RSC Adv. 4 (2014) 1378–1387.

[22] M. Mar, M. Dubois, K. Guérin, N. Batisse, B. Simon, P. Bernard, Tuning fluorine and oxygen distribution in graphite oxifluorides for enhanced performances in primary lithium battery, Carbon 141 (2019) 6–15.

[23] A. Vyalikh, L.G. Bulusheva, G.N. Chekhova, D.V. Pinakov, A.V. Okotrub, U. Scheler, Fluorine patterning in room-temperature fluorinated graphite determined by solid-state NMR and DFT, J. Phys. Chem. C 117 (2013) 7940–7948.

[24] I.P. Asanov, L.G. Bulusheva, M. Dubois, N.F. Yudanov, A.V. Alexeev, T.L. Makarova, et al., Graphene nanochains and nanoislands in the layers of room-temperature fluorinated graphite, Carbon 59 (2013) 518–519.

[25] Yu.V. Lavskaya, L.G. Bulusheva, A.V. Okotrub, N.F. Yudanov, D.V. Vyalikh, A. Fonseca, Comparative study of fluorinated single- and few-wall carbon nanotubes by X-ray photoelectron and X-ray absorption spectroscopy, Carbon 47 (2009) 1629–1636.

[26] L.G. Bulusheva, Y.V. Fedoseeva, E. Flahaut, J. Rio, C.P. Ewels, V.O. Koroteev, et al., Effect of the fluorination technique on the surface-fluorination patterning of double-walled carbon nanotubes, Beilstein J. Nanotechnol. 8 (2017) 1688–1698.

[27] L.G. Bulusheva, Yu.V. Fedoseeva, A.V. Okotrub, E. Flahaut, I.P. Asanov, V.O. Koroteev, et al., Stability of fluorinated double-walled carbon nanotubes produced by different fluorination techniques», Chem. Mater. 22 (2010) 4197–4203.

[28] C. Struzzi, M. Scardamaglia, N. Reckinger, H. Sezen, M. Amati, L. Gregoratti, et al., Probing plasma fluorinated graphene via spectromicroscopy, Phys. Chem. Chem. Phys. 19 (2017) 31418–31428.

[29] Yu.V. Fedoseeva, L.G. Bulusheva, A.V. Okotrub, D.V. Vyalikh, A. Fonseca, High reactivity of carbon nanotubes and fluorinated carbon nanotubes irradiated by Ar^+ ions, Phys. Status Solidi B 247 (2010) 2691–2694.

[30] Yu.V. Fedoseeva, L.G. Bulusheva, A.V. Okotrub, D.V. Vyalikh, A. Fonseca, A comparative study of argon ion irradiated pristine and fluorinated single-wall carbon nanotubes, J. Chem. Phys. 133 (2010) 224706.

[31] K.A. Wepasnick, B.A. Smith, K.E. Schrote, H.K. Wilson, S.R. Diegelmann, D. Howard Fairbrother, Surface and structural characterization of multi-walled carbon nanotubes following different oxidative treatments, Carbon 49 (2011) 24–26.

[32] I. Suarez-Martinez, C. Bittencourt, X. Ke, A. Felten, J.J. Pireaux, J. Ghijsen, et al., Probing the interaction between gold nanoparticles and oxygen functionalized carbon nanotubes, Carbon 47 (2009) 1549–1554.

[33] A.V. Okotrub, N.F. Yudanov, I.P. Asanov, D.V. Vyalikh, L.G. Bulusheva, Anisotropy of chemical bonding in semifluorinated graphite C_2F revealed with angle-resolved X-ray absorption spectroscopy, ACS Nano 22 (2013) 65–74.

[34] Z. Qian, J. Ma, J. Zhou, P. Lin, C. Chen, J. Chen, et al., Facile synthesis of halogenated multi-walled carbon nanotubes and their unusual photoluminescence, J. Mater. Chem. 22 (2012) 22113–22119.

[35] Z. Qian, J. Zhou, J. Ma, X. Shan, C. Chen, J. Chen, et al., The visible photoluminescence mechanism of oxidized multi-walled carbon nanotubes: an experimental and theoretical investigation, J. Mater. Chem. C 1 (2013) 307–314.

[36] L. Minati, G. Speranza, I. Bernagozzi, S. Torrengo, L. Toniutti, B. Rossi, et al., Investigation on the electronic and optical properties of short oxidized multiwalled carbon nanotubes, J. Phys. Chem. C 114 (2010) 11068–11073.

[37] E. Flahaut, R. Bacsa, A. Peigney, Ch. Laurent, Gram-scale CCVD synthesis of double-walled carbon nanotubes, Chem. Commun. 12 (2003) 1442–1443.

[38] S. Osswald, E. Flahaut, Y. Gogotsi, In situ Raman spectroscopy study of oxidation of double- and single-wall carbon nanotubes, Chem. Mater. 18 (2006) 1525–1533.

[39] E.V. Lobiak, L.G. Bulusheva, E.O. Fedorovskaya, Y.V. Shubin, P.E. Plyusnin, P. Lonchambon, et al., One–step chemical vapor deposition synthesis and supercapacitor performance of nitrogen–doped porous carbon–carbon nanotube hybrids, Beilstein J. Nanotechnol. 8 (2017) 2669–2679.

[40] T. Bortolamiol, P. Lukanov, A.-M. Galibert, B. Soula, P. Lonchambon, L. Datas, et al., Double-walled carbon nanotubes: Quantitative purification assessment, balance between purification and degradation and solution filling as an evidence of opening, Carbon 78 (2014) 79–90.

[41] N.F. Yudanov, A.V. Okotrub, YuV. Shubin, L.I. Yudanova, L.G. Bulusheva, A.L. Chuvilin, et al., Fluorination of arc-produced carbon material containing multiwall nanotubes, Chem. Mater. 14 (2002) 1472–1476.

[42] A.D. Becke, Density-functional thermochemistry. III. The role of exact exchange, J. Chem. Phys. 98 (1993) 5648–5652.

[43] C. Lee, W. Yang, R.G. Parr, Development of the Colle-Salvetti correlation-energy formula into a functional of the electron density, Phys. Rev. B 37 (1988) 785–789.

[44] Jaguar, Version 9.2, Schrödinger, LLC, New York, NY, U.S.A., 2016.

[45] W.H.E. Schwarz, Interpretation of the core electron excitation spectra of hydride molecules and the properties of hydride radicals, Chem. Phys. 11 (1975) 217–228.

[46] Yu.V. Fedoseeva, L.G. Bulusheva, A.V. Okotrub, I.P. Asanov, S.I. Troyanov, D.V. Vyalikh, Electronic structure of the chlorinated fullerene $C_{60}Cl_{30}$ studied by quantum-chemical modeling of X-ray absorption spectra, Int. J. Quantum Chem. 111 (2011) 2688–2695.

[47] L.G. Bulusheva, A.V. Okotrub, Yu.V. Lavskaya, D.V. Vyalikh, U. Dettlaff-Weglikowska, A. Fonseca, et al., Comparative NEXAFS examination of single-wall carbon nanotubes produced by different methods, Phys. Status Solidi B 246 (2009) 2637–2640.

[48] Y.S. Lee, T.H. Cho, B.K. Lee, J.S. Rho, K.H. An, Y.H. Lee, Surface properties of fluorinated single-walled carbon nanotubes, J. Fluor. Chem. 120 (2003) 99–104.

[49] M.S. Dresselhaus, G. Dresselhaus, A. Jorio, A.G. Souza Filho, R. Saito, Raman spectroscopy on isolated single wall carbon nanotubes, Carbon 40 (2002) 2043–2061.

[50] D. Levshov, T.X. Than, R. Arenal, V.N. Popov, R. Parret, M. Paillet, et al., Experimental evidence of a mechanical coupling between layers in an individual double-walled carbon nanotube, Nano Lett. 11 (2011) 4800–4808.

[51] L.G. Moura, M.V.O. Moutinho, P. Venezuela, F. Mauri, A. Righi, M.S. Strano, et al., The double-resonance Raman spectra in single-chirality *(n,* m) carbon nanotubes, Carbon 117 (2017) 41–45.

[52] P. Puech, E. Flahaut, A. Bassil, T. Juffmann, F. Beuneu, W.S. Bacsa, Raman bands of double-wall carbon nanotubes: comparison with single- and triple-wall carbon nanotubes, and influence of annealing and electron irradiation, J. Raman Spectrosc. 38 (2007) 714–720.

[53] Y. Stubrov, A. Nikolenko, V. Gubanov, V. Strelchuk, Manifestation of structure of electron bands in double-resonant Raman Spectra of single-walled carbon nanotubes, Nanoscale Res. Lett. 11 (2016) 2.

[54] R. Blume, D. Rosenthal, J.P. Tessonnier, H. Li, A. Knop-Gericke, R. Schlçgl, Characterizing graphitic carbon with X-ray photoelectron spectroscopy: a step-by-step approach, Chem. Cat. Chem. 7 (2015) 2871–2881.

[55] P.K. Chu, L. Li, Characterization of amorphous and nanocrystalline carbon films, Mat. Chem. Phys. 96 (2006) 253–277.

[56] Yu.V. Fedoseeva, G.A. Pozdnyakov, A.V. Okotrub, M.A. Kanygin, Yu.V. Nastaushev, O.Y. Vilkov, et al., Effect of substrate temperature on the structure of amorphous

oxygenated hydrocarbon films grown with a pulsed supersonic methane plasma flow, Appl. Surf. Sci. 385 (2016) 464–471.

[57] M. Krysak, B. Parekh, T. Debies, R.A. Dileo, B.J. Landi, R.P. Raffaelle, et al., Gas-phase surface functionalization of multiwalled carbon nanotubes with vacuum UV photooxidation, J. Adhes. Sci. Technol. 21 (2012) 999–1007.

[58] J. Zhang, H. Zou, Q. Qing, Y. Yang, Q. Li, Z. Liu, et al., Effect of chemical oxidation on the structure of single-walled carbon nanotubes, J. Phys. Chem. B 107 (2003) 3712–3718.

[59] O.A. Gurova, V.E. Arhipov, V.O. Koroteev, T.Y. Guselnikova, I.P. Asanov, O.V. Sedelnikova, et al., Purification of single-walled carbon nanotubes using acid treatment and magnetic separation, Phys. Status Solidi B (2019) 1800742.

[60] K.A. Worsley, I. Kalinina, E. Bekyarova, R.C. Haddon, functionalization and dissolution of nitric acid treated single-walled carbon nanotubes, J. Am. Chem. Soc. 131 (2009) 18153–18158.

[61] L. Shao, G. Tobias, C.G. Salzmann, B. Ballesteros, S.Y. Hong, A. Crossley, et al., Removal of amorphous carbon for the efficient sidewall functionalisation of single-walled carbon nanotubes, Chem. Commun. (2007) 5090–5092.

[62] H. Touhara, J. Inahara, T. Mizuno, Y. Yokoyama, S. Okanao, K. Yanagiuch, et al., Property control of new forms of carbon materials by fluorination, J. Fluor. Chem. 114 (2000) 181–188.

[63] Y. Sato, K. Itoh, R. Hagiwara, T. Fukunaga, Y. Ito, On the so-called "semi-ionic" C-F bond character in fluorine–GIC, Carbon 42 (2004) 3243–3249.

[64] P. Wang, H. Wang, W. Yang, Anomalous high adsorption energy of H_2O on fluorinated graphenes: A first principles study, Phys. Chem. Chem. Phys. 16 (2014) 20464–20470.

[65] Y.V. Fedoseeva, A.V. Okotrub, I.P. Asanov, D.V. Pinakov, G.N. Chekhova, V.A. Tur, et al., Nitrogen inserting in fluorinated graphene via annealing of acetonitrile intercalated graphite fluoride, Phys. Status Solidi B 251 (2014) 2530–2535.

[66] A. Kuznetsova, I. Popova, J.T. Yates, M.J. Bronikowski Jr, C.B. Huffman, J. Liu, et al., Oxygen-containing functional groups on single-wall carbon nanotubes: NEXAFS and vibrational spectroscopic studies, J. Am. Chem. Soc. 123 (2001) 10699–10704.

Supporting information

Preferred attachment of fluorine near oxygen-containing groups on the surface of double-walled carbon nanotubes

Yu. V. Fedoseeva[1,2], L. G. Bulusheva[1,2], V.O. Koroteev[1,2], J.-Y. Mevellec[3], B.V. Senkovskiy[4,5], E. Flahaut[6], A. V. Okotrub[1,2]

[1]Nikolaev Institute of Inorganic Chemistry SB RAS, 3 Acad. Lavrentiev Ave., 630090 Novosibirsk, Russia

[2]Novosibirsk State University, 2 Pirogova Str., 630090 Novosibirsk, Russia

[3]Institut des Matériaux Jean-Rouxel (IMN), CNRS–UMR 6502, Université de Nantes, 2 rue de la Houssinière, BP 32229, 44322 Nantes Cedex 3, France

[4]St. Petersburg State University, 7-9, Universitetskaya Nab., St. Petersburg 199034, Russia

[5]II Physikalisches Institut, Universität zu Köln, Zülpicher Straße 77, 50937 Köln, Germany

[6]CIRIMAT, Université de Toulouse, CNRS, INPT, UPS, UMR CNRS-UPS-INP N°5085, Université Toulouse 3 Paul Sabatier, Bât. CIRIMAT, 118, route de Narbonne, 31062 Toulouse cedex 9, France

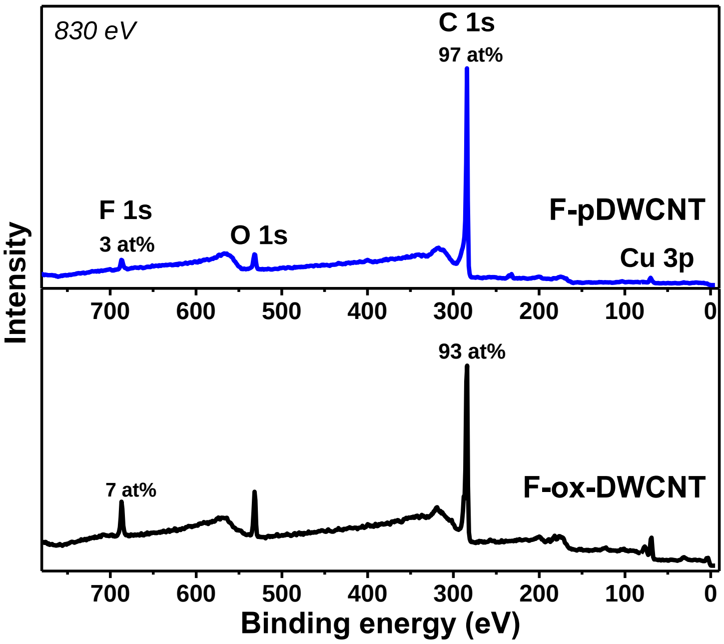

Fig. S1. XPS overall spectra of F-pDWCNTs and F-ox-DWCNTs

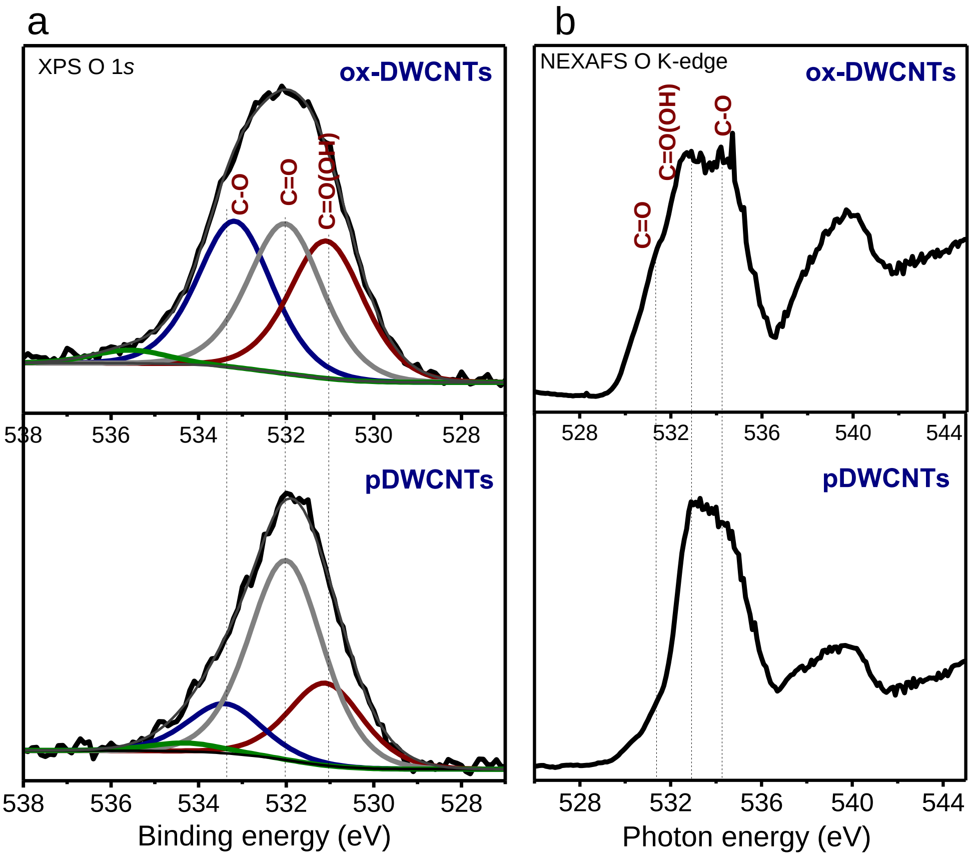

Fig. S2. XPS O1s spectra (a) and NEXAFS OK-edge spectra (b) of pDWCNTs and ox-DWCNTs